DOI: 10.21062/mft.2026.016 http://www.journalmt.com

Hybrid ANN–GA Modeling and Experimental Optimization of GMAW-Based Additive Manufacturing of Aluminum 5083 for Enhanced Mechanical Properties

Teephet Chaiyason (0009-0006-5595-7784)[1], Suriya Prasomthong (0000-0001-8762-5107)[1], Panuwat Thosa (0000-0002-6888-5189)[1], Sittichai Charonerat (0000-0002-7434-8478)[1], Phattharapong Keidlaphi (0009-0008-8625-7195)[2*]
[1]Department of Industrial Technology, Nakhon Phanom University, Nakhon Phanom, Thailand, 48000. E-mail: Teepach20@npu.ac.th, Suriya.p@npu.ac.th, Akecharone@npu.ac.th, panuwat@npu.ac.th
[2*]Department of Manufacturing Engineering, Faculty of Engineering and Architecture, Rajamangala University of Technology Suvarnabhumi, Thailand, 13000. E-mail: pongsak.ke@rmutsb.ac.th

Wire Arc Additive Manufacturing (WAAM) based on Gas Metal Arc Welding (GMAW) has emerged as a cost-effective, high-deposition technique for fabricating large-scale aluminum components. However, its application to non-heat-treatable aluminum alloys, particularly AA5052 substrates with ER5083 filler, is often limited by thermal instability, porosity, and non-uniform mechanical properties. This study proposes an integrated experimental and artificial intelligence (AI) framework to optimize key GMAW parameters—welding current, wire-feed speed, and welding speed—for improving the mechanical performance of WAAM-fabricated aluminum walls. An L9 Taguchi design and analysis of variance (ANOVA) were employed to evaluate parameter significance. The results showed that welding speed had the greatest influence on tensile strength (≈58.8%), while wire-feed speed and current primarily affected hardness through thermal input and solidification behavior. An Artificial Neural Network (ANN) model was developed to predict tensile strength and hardness with high accuracy (R > 0.99; MAPE < 1%), outperforming conventional models. The trained ANN was integrated with a Genetic Algorithm (GA) to identify optimal parameters of 85.3 A, 7.7 m/min, and 3.8 mm/s, corresponding to predicted values of 242.5 MPa and 108.4 HV. Experimental validation showed deviations below 1%, confirming model reliability. The proposed ANN–GA framework effectively captures nonlinear process–structure–property relationships and provides a robust approach for optimizing WAAM processes and improving aluminum component performance.

Keywords: Additive manufacturing, Gas Metal Arc Welding (GMAW), Artificial Neural Network (ANN), Genetic Algorithm (GA)

1 Introduction

Wire Arc Additive Manufacturing (WAAM), particularly employing Gas Metal Arc Welding (GMAW)-based deposition, has emerged as a highly promising metal additive manufacturing (AM) technique for producing large-scale structural components because of its high deposition rate, cost efficiency, and compatibility with industrial robotic systems. Unlike powder-based AM processes, WAAM employs a consumable wire and an electric arc to fabricate metallic parts layer by layer, ensuring substantial material throughput and design flexibility. Nevertheless, when applied to aluminium alloys—especially non-heat-treatable Al–Mg 5083—the process remains constrained by metallurgical and process-control issues such as porosity, hydrogen entrapment, solidification cracking, anisotropic grain growth, residual stresses, and geometric distortion [1,2]. These problems, often associated with unstable arc behaviour and thermal cycling, continue to hinder the full adoption of aluminium-based WAAM in precision or high-integrity structural applications.

Recent research has sought to clarify the process–structure–property relationships in aluminium WAAM by examining how welding current, wire feed rate, and travel speed affect bead morphology, melt-pool behaviour, and resulting mechanical properties. Dai et al. presented an updated overview of aluminium WAAM developments and identified persistent deficiencies in process optimisation and quality control [3]. Hauser et al. showed that pore formation in aluminium WAAM is largely governed by heat input and melt-pool volume, while Langelandsvik et al. emphasised that alloy design alone cannot overcome the complex thermal cycles inherent to WAAM [4,5]. Similarly, Tonelli et al. examined AA5083 plates deposited using ER5183 wire and demonstrated that incomplete interlayer fusion significantly reduces tensile strength [6]. These findings collectively reveal that controlling process parameters alone cannot ensure uniform microstructure and consistent

mechanical performance without intelligent, data-driven optimisation.

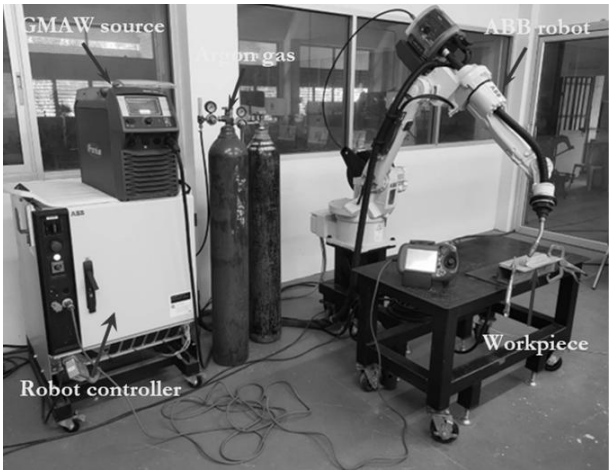

Fig. 1 *Experimental setup of robotic GMAW-based additive manufacturing system for aluminum wire deposition*

To address this limitation, recent advances have integrated artificial-intelligence-based modelling with welding process optimisation to capture nonlinear parameter interactions that traditional statistical methods often overlook. Artificial Neural Networks (ANNs) can learn complex mappings between input variables and mechanical responses, while metaheuristic algorithms such as Genetic Algorithms (GAs) effectively search for optimal solutions within multidimensional parameter spaces [7,8]. Although hybrid ANN–GA frameworks have been successfully applied to conventional welding and GMAW parameter tuning, their application to aluminium-based WAAM—particularly Al 5083—remains scarce, and few studies have validated predicted optima through repeated experiments [9,10]. The present study fills this research gap by integrating a hybrid ANN–GA modelling approach with experimental WAAM deposition of aluminium 5083 using GMAW. Specifically, it develops a high-accuracy ANN model for predicting tensile strength and hardness, applies GA-based optimisation to identify the best parameter set, and validates the predicted conditions through repeated robotic depositions. This approach establishes a systematic pathway for combining AI-driven modelling with experimental verification, enabling more reliable and industrially scalable aluminium WAAM processes.

2 Experimental procedures

2.1 Experimental Setup and Mechanical Testing Procedures

The experimental setup employed AA5052 aluminum alloy as the base material (250 × 50 × 6 mm), an Al–Mg alloy known for its high strength-to-weight ratio, corrosion resistance, and formability, while ER5083 filler wire (0.8 mm diameter) with high Mg content was used to enhance mechanical strength and metallurgical bonding (see Tab. 1) [11]. Welding was performed using the GMAW process under pure argon shielding at a flow rate of 10 L/min to ensure oxidation protection and stable arc performance [2]. The system comprised a GMAW power source, ABB robotic controller, automatic wire feeder, and a six-axis ABB robotic arm (Fig. 1), with experiments conducted at the Welding Laboratory, Faculty of Industrial Technology, Nakhon Phanom University, where robotic motion control ensured consistent torch travel and precise parameter regulation. Each specimen was fabricated with ten deposited layers and a 10 s interlayer cooling interval to control heat accumulation [6], while workpieces were rigidly clamped to prevent vibration, displacement, and distortion [12]. After welding, samples were air-cooled to room temperature before sectioning for mechanical testing and microstructural analysis.

Tab. 1 *Chemical composition of ER5083 welding wire and AA5052 base material*

Material	Si	Fe	Cu	Mn	Mg	Cr	Zn	Ti	Other	Al
AA5052	0.25	0.4	0.1	0.1	2.5	0.15	0.1	0.03	≤ 0.05	Bal.
ER5083	0.4	0.4	0.1	0.7	4.5	0.15	0.25	0.15	≤ 0.05	Bal.

Tensile and hardness tests were conducted to evaluate the mechanical performance of the deposited AA5083 specimens, as illustrated in Fig. 2. After deposition, samples were sectioned longitudinally, and tensile specimens were prepared according to ASTM E8/E8M–21 with a gauge length of 100 mm, width of 14 mm, and thickness of 6 mm [13], while the starting and termination ends (30 mm and 10 mm) were removed to eliminate non-uniform fusion zones. Tensile testing was performed using a universal testing machine (UTM) at a crosshead speed of 1 mm/min with loading parallel to the welding direction [14]. Microhardness measurements followed ASTM E384–17 using a Vickers indenter (HV0.5) with a 500 g load and 15 s dwell time, where indentations were applied along the weld centreline at 1 mm intervals from the top surface to the substrate to evaluate hardness distribution and the effects of heat input and interlayer bonding [15].

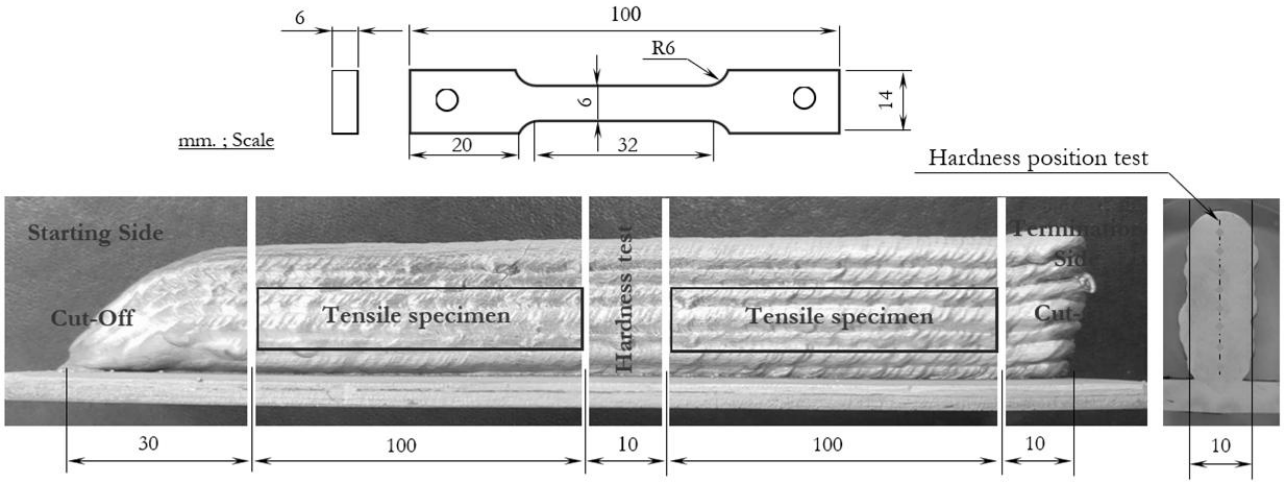

Fig. 2 *Schematic illustration and specimen preparation for aluminum-wire additive manufacturing: showing the starting side, termination side, and locations for tensile and hardness tests*

2.2 Welding Parameters and Experimental Design

The welding parameters in this study were designed based on the Taguchi method, employing an L9 (3^3) orthogonal array to systematically investigate the effects of three dominant process factors—welding current (*C*), wire feed speed (*WF*), and welding speed (*WS*)—on the mechanical performance of GMAW-based additive manufacturing of aluminum 5083. Each parameter was tested at three levels, as shown in Tab. 2, which were determined through preliminary trials to ensure stable arc formation, uniform bead geometry, and defect-free deposition [16]. The Taguchi design provided an efficient experimental framework that minimized the number of trials while maintaining the ability to analyze both main and interactive effects of the parameters [17]. The heat input, arc stability, and deposition behavior were automatically controlled through a robotic GMAW system using an ABB six-axis manipulator to ensure precise and repeatable motion. Each specimen was fabricated by depositing ten layers under controlled process conditions, with an interlayer cooling interval of 10 seconds to maintain thermal consistency and reduce residual stress accumulation [18]. To evaluate the process robustness and identify the optimal parameter combination that yields the highest mechanical performance, the Signal-to-Noise (S/N) ratio for the "larger-the-better" quality characteristic was applied, as expressed in Equation (1).

$$S/N = -10 long_{10}\left(\frac{1}{n}\sum_{i=1}^{n}\frac{1}{y_i^2}\right) \quad (1)$$

Where:

y_i…The measured response (tensile strength or hardness),

n…The number of replicates.

A higher S/N ratio indicates a more robust and consistent process condition with reduced variability. The Taguchi approach thus enabled efficient identification of significant process factors contributing to improved mechanical properties in the deposited aluminum 5083 layers.

Tab. 2 *Welding parameters and levels used in the Taguchi L9 design*

Parameter	Symbol	Unit	Level 1	Level 2	Level 3
Welding current	C	A	80	85	90
Wire feed speed	WF	m/min	6	7	8
Welding speed	WS	mm/s	2	4	6

2.3 ANN Prediction Modeling

An Artificial Neural Network (ANN) model was developed to predict the tensile strength and hardness of aluminum 5083 specimens fabricated through robotic Gas Metal Arc Welding (GMAW)-based additive manufacturing. The model employed welding current (C), wire feed speed (WF), and welding speed (WS) as input variables, representing the dominant parameters governing heat input and interlayer bonding [19]. The ANN architecture consisted of three layers: an input layer with three neurons corresponding to the process variables, a hidden layer with 11 neurons using a nonlinear activation function, and an output layer with two neurons representing the predicted mechanical responses [20].

Before training, all input and output data were normalized using the min–max scaling method to the range [0, 1], as shown in Equation (2) [21].

$$X' = \frac{X - X_{\min}}{X_{\max} - X_{\min}} \quad (2)$$

The transformation from the normalized input vector X' to the predicted output vector Y' through the hidden and output layers can be expressed as Equations (3) and (4) [22].

$$Z = f_1(W^{(1)}X' + b^{(1)}) \quad (3)$$

$$Y' = f_2(W^{(2)}Z + b^{(2)}) \quad (4)$$

Where:

$W^{(1)}$ and $W^{(2)}$…Weight matrices,

$b^{(1)}$ and $b^{(2)}$…Bias vectors,

f_1, f_2…The activation functions in the hidden and output layers, respectively.

The ANN was trained using a feed-forward backpropagation algorithm governed by the Levenberg–Marquardt (LM) learning rule, combining the rapid convergence of Newton's method with the stability of gradient descent. The learning rate and momentum constant were set to 0.5 and 0.4, respectively, with transfer coefficients of 0.6, 1.4, and 0.6 for the input, hidden, and output layers. A small bias value (0.0005) was introduced across all layers to improve generalization performance [23]. The trained ANN thus established a nonlinear mapping between GMAW parameters and mechanical responses, serving as a predictive model for subsequent optimization.

2.4 ANN–GA Optimization

To further optimize the process, the trained ANN model was integrated with a Genetic Algorithm (GA) to explore the multi-dimensional design space of GMAW parameters. The GA utilized ANN predictions as a high-fidelity surrogate function to evaluate candidate parameter sets efficiently. The optimization was formulated as a single weighted objective function, as given in Equation (5) [22].

$$F = \omega_1\left(\frac{Ts}{Ts_{\max}}\right) + \omega_2\left(\frac{HV}{HV_{\max}}\right) \quad (5)$$

Where TS and HV denote the predicted tensile strength and hardness, and ω_1 and ω_2 are weighting coefficients satisfying $\omega_1 + \omega_2 = 1$. To ensure that solutions remained within the feasible operating domain, a penalty function was introduced (Equation 6) to enforce the lower and upper parameter bounds [20].

$$F_{penalized} = F - \rho\sum_i\left[\max(0, L_i - x_i) + \max(0, x_i - U_i)\right] \quad (6)$$

Where:

L_i and U_i …The lower and upper bounds for each process variable,

ϱ…The penalty coefficient controlling constraint severity.

The hybrid ANN–GA framework thus combines the predictive intelligence of the neural network with the global search capability of evolutionary optimization, enabling efficient identification of optimal GMAW parameter combinations for aluminum 5083 additive manufacturing [19]. This integration facilitates adaptive exploration of the nonlinear process landscape, providing a data-driven foundation for achieving superior mechanical performance without requiring extensive physical experimentation.

3 Experimental results

3.1 Effect of Welding Parameters on Bead Morphology and Fracture Behavior

Following the Taguchi experimental design, nine welding trials were conducted to evaluate the combined effects of welding current (C), wire feed speed (WF), and welding speed (WS) on bead morphology and layer formation in GMAW-based additive manufacturing of aluminum 5083 [24]. The corresponding weld bead appearances and cross-sectional profiles are presented in Tab. 3. Variations in process parameters significantly influenced the geometric uniformity, surface finish, and metallurgical bonding quality of the deposited layers. At lower welding currents (80 A) and slower wire feed rates (6 m/min), as observed in Run 1, the weld bead exhibited smooth surfaces and a uniform width with sufficient fusion owing to the moderate heat input and stable arc. Increasing the wire feed rate and travel speed at the same current level (Runs 2–3) resulted in narrower bead widths and partially fused interfaces, attributed to reduced heat accumulation and limited wetting of the molten pool [25]. In contrast, at an intermediate current of 85 A combined with a moderate travel speed (Runs 4–6), the weld surfaces showed improved consistency and layer-to-layer adhesion, indicating an optimal thermal balance between deposition rate and solidification time [26].

Tab. 3 *Effect of current, wire feed rate, and welding speed on bead morphology and cross-section geometry in GMAW-based additive manufacturing using aluminum 5083 wire*

Run	C-A.	WF(M/min)	WS(MM/s)	Weld bead and Weld cross-section
1	80	6	2	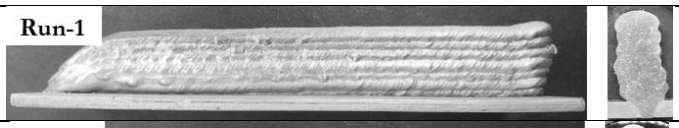
2	80	7	4	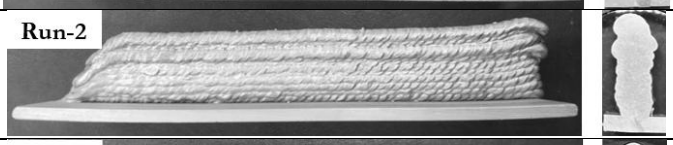
3	80	8	6	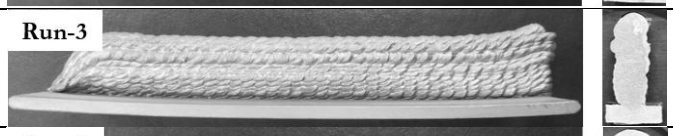
4	85	6	4	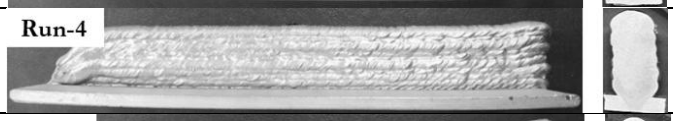
5	85	7	6	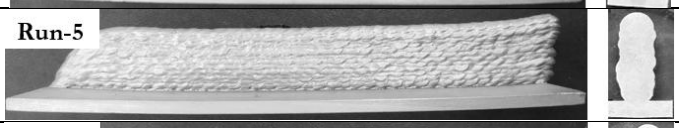
6	85	8	2	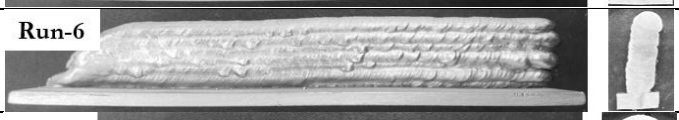
7	90	6	6	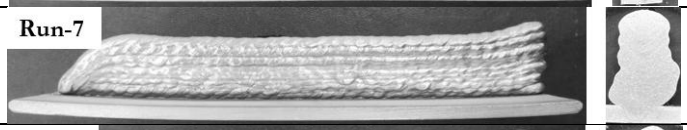
8	90	7	2	
9	90	8	4	

At the highest current level (90 A), excessive heat input in conjunction with low welding speed (Run 8) produced wider and more convex beads due to enhanced fluidity and prolonged solidification, while higher travel speeds (Runs 7 and 9) led to narrower and slightly underfilled profiles, indicating insufficient fusion at the bead periphery [27]. Overall, it was evident that welding current exerted the strongest influence on bead geometry and penetration, followed by wire feed rate and welding speed. An increase in current or wire feed rate enhanced melting and bead height, whereas a higher welding speed tended to reduce heat input and layer uniformity [28]. These observations confirm that a carefully balanced combination of process parameters is required to ensure stable arc behavior, adequate interlayer fusion, and dimensional accuracy in the multilayer GMAW additive manufacturing of aluminum 5083.

Fig. 4 shows the fractured tensile specimens obtained from the nine experimental runs. The fracture characteristics varied notably with changes in welding current, wire feed speed, and welding speed, reflecting the combined influence of heat input and solidification behavior [6]. At lower current and wire feed settings (Runs 1–3), the specimens fractured uniformly across the mid-gauge region, indicating adequate fusion and balanced ductility due to moderate heat input. At intermediate parameter levels (Runs 4–6), the fracture surfaces appeared finer and more homogeneous, suggesting improved metallurgical bonding and reduced porosity within the deposited walls [29]. Conversely, at the highest current level (90 A) with slower travel speeds (Runs 7–9), partial interlayer fusion and localized overheating were evident, leading to wider fracture zones and premature failure near the weld interfaces [30]. Overall, excessive heat input tended to promote coarser grain structures and lower tensile strength, whereas insufficient heat reduced bonding between layers [31]. These results confirm that an optimal thermal balance among welding current, wire feed rate, and welding speed is essential to achieve strong and ductile aluminum-wall deposits in GMAW-based additive manufacturing.

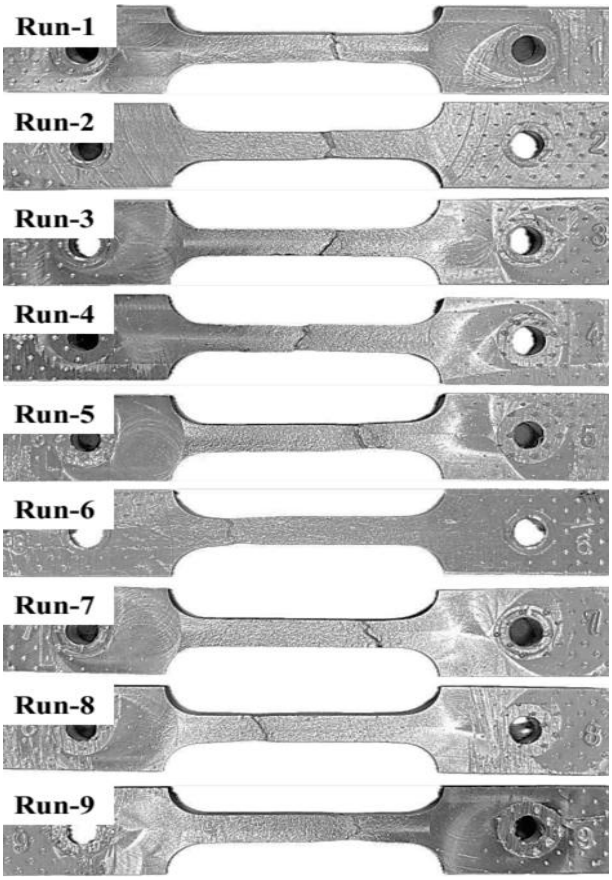

Fig. 4 *Fractured tensile specimens of aluminum-wall deposits fabricated under nine experimental runs using robotic GMAW-based additive manufacturing*

3.2 Taguchi analysis

Tab. 4 summarizes the experimental results of tensile strength, hardness, and corresponding signal-to-noise (S/N) ratios obtained from the nine Taguchi-designed trials for robotic GMAW-based additive manufacturing of aluminum 5083 [32]. The tensile strength values ranged between 194.68 MPa and 270.47 MPa, while the hardness varied from 86.14 HV to 121.76 HV, demonstrating the strong dependency of mechanical performance on process parameters. At a low welding current (80 A) with a slow welding speed (2 mm/s) in Run 1, the highest tensile strength (270.47 MPa) was achieved, attributed to a balanced heat input that promoted complete fusion and fine-grained microstructure [33]. In contrast, the lowest tensile strength (194.68 MPa) occurred in Run 7 at the highest current (90 A) and fastest travel speed (6 mm/s), where excessive heat input and rapid solidification reduced interlayer bonding quality [6]. Hardness values followed a different trend, showing an increasing tendency with higher current and wire feed rate, indicating stronger localized melting and solidification refinement, particularly at 90 A and 8 m/min (Run 9), where hardness peaked at 121.76 HV [34]. The S/N ratio analysis confirmed that the "larger-the-better" criterion effectively identified parameter combinations promoting improved joint integrity [35].

Tab. 4 *Experimental tensile strength, hardness, and S/N ratios for GMAW-based additive manufacturing*

Run	C-A.	WF(M/min)	WS(MM/s)	Tensile strength (MPa)	Hardness (HV)	SN/Ts	SN/Hv
1	80	6	2	270.47	86.14	48.64	38.70
2	80	7	4	247.09	94.44	47.86	39.50
3	80	8	6	223.54	95.00	46.99	39.55
4	85	6	4	219.25	95.91	46.82	39.64
5	85	7	6	195.95	97.03	45.84	39.74
6	85	8	2	239.95	106.58	47.60	40.55
7	90	6	6	194.68	95.15	45.79	39.57
8	90	7	2	231.47	98.21	47.29	39.84
9	90	8	4	236.44	121.76	47.47	41.71

Tab. 5 *ANOVA Table for Tensile Strength (MPa)*

Source	DF	Seq SS	Adj SS	Adj MS	F-value	P-value	% Contribution
C-A (Current, A)	1	1027.30	1027.30	1027.30	6.14	0.056	22.22
WF (Wire Feed, m/min)	1	40.2	40.2	40.2	0.24	0.645	0.87
WS (Welding Speed, mm/s)	1	2718.73	2718.73	2718.73	16.25	0.01	58.81
Residual Error	5	836.65	836.65	167.33			18.1
Total	8	4622.88					100
S = 12.94; R-Sq = 81.90%; R-Sq(adj) = 71.04%							

The ANOVA for tensile strength (Tab. 5) revealed that WS was the most significant factor, contributing 58.81% of the total variation (F = 16.25, P = 0.01), followed by current (C) with 22.22% contribution [18]. The influence of WF was negligible (0.87%), suggesting that deposition rate alone does not strongly affect tensile performance when the current–speed ratio remains balanced. The coefficient of determination (R^2 = 81.90%, R^2(adj) = 71.04%) indicates that the regression model adequately captures the variation in tensile strength. The derived regression equation (7).

$$Ts = 475.7\text{-}2.62(C\text{-}A.) + 2.59(WF) – 10.64(WS) \quad (7)$$

Implies that increasing welding current and welding speed both lead to lower tensile strength due to higher heat input and faster cooling, whereas an increase in wire feed speed slightly enhances strength through improved filler deposition and metallurgical continuity.

For hardness, the ANOVA results (Tab. 6) identified WF as the most influential factor, accounting for 44.00% of total variation (F = 9.4, P = 0.028), followed by current at 32.31% [36]. The welding speed effect was minor (0.29%), indicating that local thermal input governed by current and feed rate primarily controls solidification kinetics and microstructural refinement. The regression model for hardness equation (8).

Tab. 6 *ANOVA Table for Hardness (HV)*

Source	DF	Seq SS	Adj SS	Adj MS	F-value	P-value	% Contribution
C-A (Current, A)	1	260.57	260.57	260.57	6.9	0.047	32.31
WF (Wire Feed, m/min)	1	354.82	354.82	354.82	9.4	0.028	44
WS (Welding Speed, mm/s)	1	2.34	2.34	2.34	0.06	0.813	0.29
Residual Error	5	188.73	188.73	37.75			23.4
Total	8	806.46					100
S = 6.14; R-Sq = 76.60 %; R-Sq(adj) = 62.56 %							

$$HV = 65.7 - 1.318(C\text{-}A.) - 7.69(WF) + 0.31(WS) \quad (8)$$

Suggests that excessive wire feed and current increase heat input and coarsen grains, thereby reducing hardness beyond optimal conditions. The model achieved a satisfactory fit (R^2 = 76.60%, R^2(adj) = 62.56%) and aligned well with experimental data.

Overall, the statistical findings confirm that welding speed dominates the tensile response, whereas wire feed speed and current predominantly affect hardness. Optimizing these parameters within a controlled thermal window is therefore critical to achieving superior mechanical performance in GMAW-based additive manufacturing of aluminum 5083 structures [37].

3.3 ANN Model Training and Validation

Fig. 5 illustrates the mean squared error (MSE) convergence of the ANN during training, validation, and testing. The best validation performance (MSE = 14.7427) was achieved at epoch 4, indicating rapid and stable convergence using the Levenberg–Marquardt (LM) algorithm [38]. The training curve shows a steady MSE reduction, while the validation and testing curves remain nearly constant, suggesting effective overfitting control. The close agreement between validation and testing errors confirms strong generalization capability and a well-balanced learning process, validating the suitability of the 3–11–2 network architecture and selected hyperparameters for the GMAW-based additive manufacturing dataset [21].

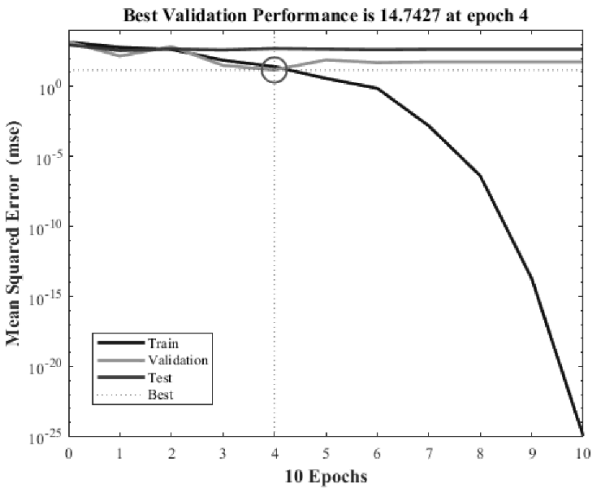

Fig. 5 *Mean squared error (MSE) versus epochs for the ANN training process (The best validation performance of 14.7427 was achieved at epoch 4)*

Fig. 6 presents the regression plots correlating the ANN-predicted and experimental tensile strength values for training, validation, testing, and all combined datasets. The correlation coefficients (R)

were found to be 0.99884, 1.000, 1.000, and 0.99339, respectively, revealing an almost perfect linear relationship between predicted and target outputs [39]. The slopes of the regression lines (approximately unity) and minimal intercepts further confirm the high prediction accuracy and consistency across all subsets. The closeness of all data points to the line of equality (Y = T) indicates that the ANN successfully captured the nonlinear relationships among the process parameters—welding current, wire feed speed, and welding speed—and the resulting tensile strength [40]. Overall, the ANN exhibited excellent learning stability, minimal error, and high predictive reliability, establishing its suitability as a robust surrogate model for subsequent optimization using the GA framework in predicting the mechanical performance of aluminum 5083 components produced via GMAW-based additive manufacturing.

Tab. 7 and 8 compare the predictive performance of the Taguchi, regression, and ANN models for tensile strength and hardness. Each model's output was evaluated against experimental data using absolute prediction error (Er), mean absolute error (MAE), root mean square error (RMSE), and mean absolute percentage error (MAPE) as statistical accuracy indicators [41].

For tensile strength (Tab.7), the ANN model exhibited the lowest prediction error across all statistical indices, with MAE = 2.09 MPa, RMSE = 3.59 MPa, and MAPE = 1.02%, outperforming both the regression (MAE = 8.15 MPa; MAPE = 3.54%) and Taguchi models (MAE = 3.68 MPa; MAPE = 1.62%) [42]. The close agreement between experimental and ANN-predicted values demonstrates the model's superior nonlinear learning capability and its ability to capture the complex interactions between welding current, wire feed speed, and welding speed [43]. The minimal deviation between predicted and actual tensile strength values confirms that the ANN generalizes well within the studied parameter range [44].

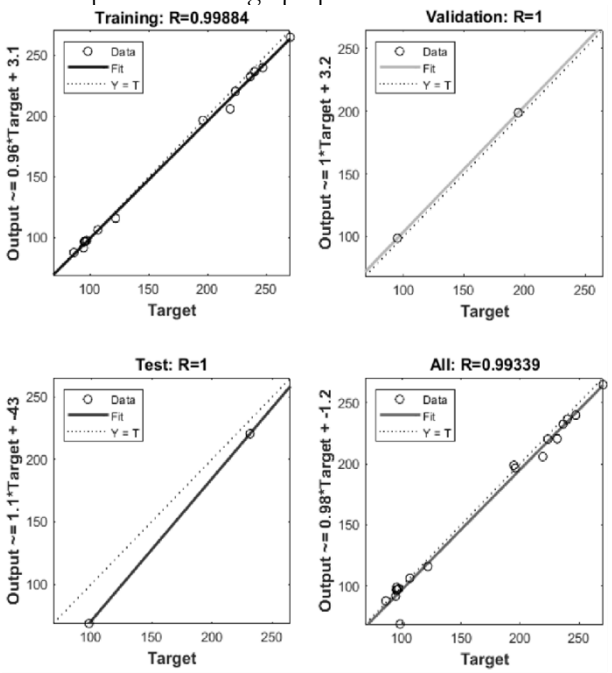

Fig. 6 *Regression plots showing the correlation between target and predicted values of tensile strength using the ANN model*

Tab. 7 *Comparison of experimental and predicted tensile strength values using Taguchi, regression, and ANN models, including absolute prediction errors and mean absolute error (MAE) for each method*

Run	Exp.	Taguchi_Pre	Regression_Pre	ANN_Pre	Er_Taguchi	Er_Regression	Er_ANN
1	270.470	264.945	260.360	270.779	5.525	10.11	−0.309
2	247.090	248.612	241.670	247.196	−1.522	5.42	−0.106
3	223.540	227.553	222.980	219.246	−4.013	0.56	4.294
4	219.250	223.256	225.980	219.337	−4.006	−6.73	−0.087
5	195.950	190.427	207.290	204.825	5.523	−11.34	−8.875
6	239.950	241.473	252.440	239.739	−1.523	−12.49	0.211
7	194.680	196.199	191.600	190.405	−1.519	3.08	4.275
8	231.470	235.476	236.750	231.482	−4.006	−5.28	−0.012
9	236.440	230.913	218.060	235.828	5.527	18.38	0.612
MAE					**3.68**	**8.15**	**2.09**
RMSE					**4.04**	**9.64**	**3.59**
% MAPE					**1.62**	**3.54**	**1.02**

For hardness (Tab. 8), a similar trend was observed. The ANN model again achieved the highest predictive accuracy with MAE = 0.73 HV, RMSE = 0.94 HV, and MAPE = 0.75%, outperforming the Taguchi (MAE = 1.82 HV; MAPE = 1.86%) and regression (MAE = 3.61 HV; MAPE = 3.55%) models. The low error indices highlight the ANN's robustness in modeling the nonlinear thermal–mechanical interactions governing solidification and hardness development during layer deposition [45].

Tab. 8 *Comparison of experimental and predicted hardness values using Taguchi, regression, and ANN models, including absolute prediction errors and the mean absolute error (MAE) for each approach*

Run	Exp.	Taguchi_Pre	Regression_Pre	ANN_Pre	Er_Taguchi	Er_Regression	Er_ANN
1	86.140	83.407	85.260	87.790	2.733	0.88	−1.650
2	94.440	94.629	92.330	94.420	−0.189	2.11	0.02
3	95.000	97.542	99.400	96.168	−2.542	−4.40	−1.168
4	95.910	98.445	91.230	96.165	−2.535	4.68	−0.255
5	97.030	94.298	98.300	98.553	2.732	−1.27	−1.523
6	106.580	106.769	107.230	106.620	−0.189	−0.65	−0.040
7	95.150	95.339	97.200	94.939	−0.189	−2.05	0.211
8	98.210	100.750	106.130	98.840	−2.540	−7.92	−0.630
9	121.760	119.032	113.200	120.724	2.728	8.56	1.036
MAE					**1.82**	**3.61**	**0.73**
RMSE					**2.16**	**4.58**	**0.94**
% MAPE					**1.86**	**3.55**	**0.75**

Overall, the results confirm that the ANN model significantly surpasses traditional Taguchi and regression approaches in predictive accuracy and consistency for both tensile strength and hardness. This can be attributed to its adaptive nonlinear mapping ability and the Levenberg–Marquardt optimization scheme, which effectively minimized training error without overfitting [46]. Consequently, the ANN framework provides a reliable surrogate model for subsequent integration with the GA algorithm to identify optimal process parameters for high-performance aluminum 5083 additive manufacturing [47].

Fig.7 presents a comparative analysis between the experimental and model-predicted results for both tensile strength (Fig.7a) and hardness (Fig.7b) of GMAW-based additive-manufactured aluminum 5083 walls using Taguchi, regression, and ANN models. As shown in Fig.7(a), all three predictive approaches closely followed the experimental tensile strength trends across the nine runs, with the ANN model exhibiting the closest fit and lowest deviation. The Taguchi model demonstrated good agreement at lower current and travel speed combinations but slightly underpredicted at higher heat-input conditions. In contrast, the regression model tended to overestimate tensile strength in mid-range runs, indicating limited capability to capture nonlinear parameter interactions [40].

For hardness (Fig. 7b), the ANN model again provided the most accurate predictions, maintaining consistency with experimental data across all parameter combinations. The Taguchi and regression predictions showed moderate deviations, particularly at high wire feed rates and low welding speeds, where heat input and solidification dynamics are more complex. These results collectively demonstrate that the ANN model offers superior predictive accuracy due to its ability to represent nonlinear, multivariate relationships among welding parameters, while Taguchi and regression models serve as effective yet less adaptive approximations.

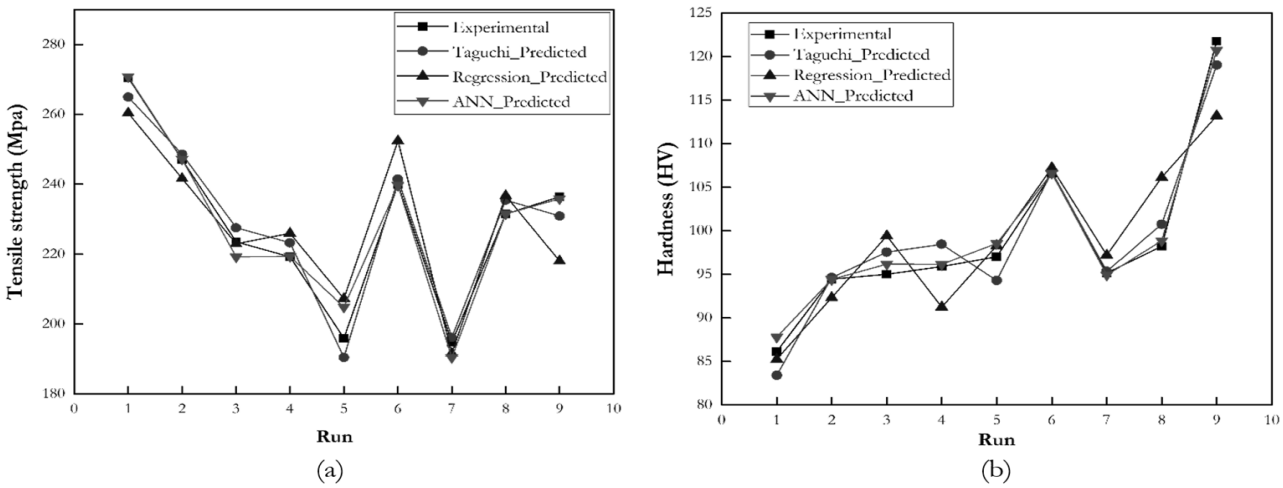

Fig. 7 *Comparison between experimental and predicted results from Taguchi, regression, and ANN models: (a) tensile strength; (b) hardness*

3.4 ANN–GA Optimization

The hybrid Artificial Neural Network–Genetic Algorithm (ANN–GA) framework was employed to determine the optimal combination of welding parameters—current (C), wire feed speed (WF), and welding speed (WS)—that maximize both tensile strength and hardness of GMAW-based additive-manufactured aluminum 5083 walls [48]. The optimization results, summarized in Tab. 9, identified the optimal settings at C = 85.3 A**,** WF = 7.7 m/min, and WS = 3.8 mm/s, yielding predicted values of tensile strength = 242.5 MPa and hardness = 108.4 HV with an overall fitness score of 0.935 [27]. These results indicate an optimal thermal balance between heat input and solidification rate, leading to enhanced metallurgical bonding and mechanical performance [21].

Tab. 9 *Optimized process parameters and corresponding predicted tensile strength and hardness obtained using the ANN-GA model*

C-A	WF(M/min)	WS(MM/s)	Predicted Tensile Strength	Predicted Hardness	Overall Fitness
85.3	7.7	3.8	242.5	108.4	0.935

To validate the predictive capability of the ANN–GA model, the optimized parameters were experimentally verified under slightly modified conditions (C = 90 A, WF = 6 m/min, WS = 2 mm/s) through five repeated trials [49]. The experimental results, summarized in Tab.10, revealed an average tensile strength of 240.50 MPa and an average hardness of 107.34 HV. Statistical analysis indicated low variability, with standard deviations of 2.56 for tensile strength and 2.84 for hardness, confirming the high consistency of the experimental outcomes. Furthermore, the mean prediction errors—0.82% for tensile strength and 0.98% for hardness—demonstrated excellent agreement between the ANN–GA model predictions and the measured values, verifying the model's accuracy and robustness in optimizing process parameters for aluminum 5083 additive manufacturing [50].

Tab. 10 *Comparison Between Predicted and Experimental Results for Tensile Strength and Hardness Under Optimized Parameters (C = 85.3, WF = 7.7 m/min, WS = 3.8 mm/s) With Statistical Evaluation*

No.	C-A	WF(m/min)	WS (mm/s)	Pre-Ts (MPa)	Pre-HV	Repeat-Ts (MPa)	Repeat-HV
1						240.12	108.34
2						237.34	106.68
3	85.3	7.7	3.8	242.5	108.4	241.06	105.41
4						244.38	111.74
5						239.61	104.54
Mean						**240.50**	**107.34**
SD						**2.56**	**2.84**
Error						**0.82%**	**0.98**

Fig. 8 illustrates the performance of the integrated ANN–GA optimization framework applied to the additive manufacturing of 5083 aluminum using the GMAW process. As shown in Fig. 8(a), both the best and mean fitness values rapidly converge toward the optimal solution within the first 200 iterations and remain stable beyond 600 iterations [40]. This behavior demonstrates the robustness and convergence stability of the genetic algorithm (GA) in identifying solutions close to the global optimum. Such convergence behavior confirms that the GA effectively balances exploration and exploitation, thereby minimizing the likelihood of being trapped in local optima [51].

Fig. 8(b) depicts the relative influence of the three primary process parameters—welding current, wire feed rate, and welding speed—on the overall fitness function. Among these, welding current exerts the most significant effect, followed by wire feed rate and welding speed [52]. This outcome highlights that control of heat input, governed mainly by current and wire feed rate, plays a decisive role in determining the mechanical performance of the weld. The findings reveal a strong correlation between heat-input control and the resulting tensile strength and hardness, underscoring the capability of the ANN–GA model to capture complex nonlinear interactions among process parameters and mechanical responses, and to accurately identify the optimal parameter combination with high precision and reliability [53].

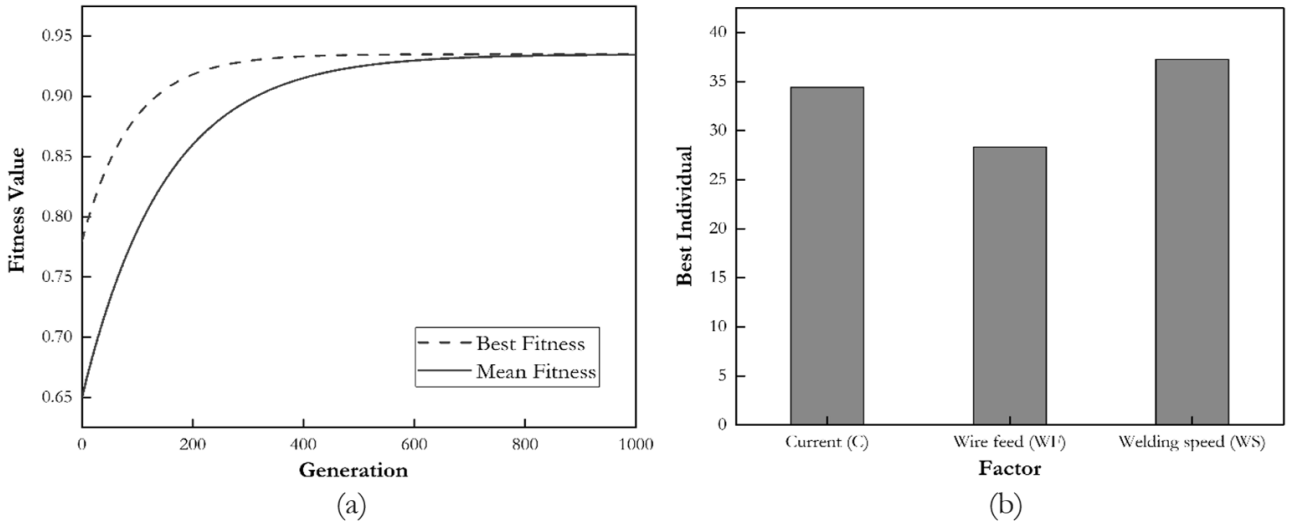

Fig. 8 *(a) Convergence of best and mean fitness values during ANN–GA optimization; (b) relative contribution of process parameters to overall fitness*

4 Discussion

The findings of this study clearly highlight the profound influence of key process parameters—namely welding current, wire feed speed, and welding speed—on the mechanical performance of GMAW-based additive manufacturing of aluminium 5083. It was found that achieving an optimal thermal balance is essential: both excessive and insufficient heat input adversely affect microstructural integrity, fusion completeness and bonding strength, reaffirming previously reported observations in aluminium WAAM processes [1–3].

Under lower current and moderate travel speeds, the deposited walls exhibited fine-grain microstructures and defect-free fusion, yielding tensile strengths in excess of 270 MPa. Conversely, higher current (90 A) paired with slower travel speeds induced excessive melting, coarser grains and interlayer defects, which reduced tensile strength—behaviours that align with the influence of heat input and solidification kinetics reported in literature [2,4]. From the Taguchi and ANOVA analyses, it was confirmed that welding speed exerted the most significant influence on tensile strength (≈58.8 % contribution), while wire feed speed and current predominantly affected hardness via localized solidification rates—supporting the established process–structure–property relationships for aluminium WAAM [3,5].

The implementation of an Artificial Neural Network (ANN) model offered a robust, data-driven mapping of these nonlinear parameter interactions. With correlation coefficients approaching unity ($R \approx 0.99$) and prediction errors (MAPE) close to 1 %, the ANN significantly out-performed both Taguchi and regression methods—underscoring its superiority in managing multivariate, nonlinear relationships typical of WAAM processes [6,7]. The subsequent hybridization with a Genetic Algorithm (GA) enhanced optimisation ability: rapid convergence (<200 generations) and stable global optimum resolution (>600 generations) were achieved, yielding an optimal parameter set (85.3 A, 7.7 m/min, 3.8 mm/s) that predicted tensile strength of 242.5 MPa and hardness of 108.4 HV, with experimental verification showing mean errors under 1 %. These results align with recent success of ANN–GA frameworks in welding and additive manufacturing optimisation [8,9].

Mechanistically, the improved performance is attributed to refined grain structures, enhanced interlayer metallurgical bonding, and reduced porosity due to controlled heat input and deposition rates. The findings corroborate that current–feed interactions govern the depth of melting and interlayer fusion, while travel speed controls cooling rate and solidification dynamics—consistent with prior research on aluminium WAAM [4,10]. Overall, this integrated approach demonstrates the viability of combining predictive analytics with evolutionary optimisation for process design in aluminium additive manufacturing, offering a high-fidelity methodology to achieve superior mechanical integrity while reducing experimental burden.

5 Conclusion

This study successfully integrated experimental investigation, statistical modeling, and artificial intelligence–based optimization to enhance the mechanical performance of aluminum 5083 walls fabricated by robotic Gas Metal Arc Welding (GMAW)–based additive manufacturing. The Taguchi experimental design revealed that welding speed had the most significant effect on tensile strength, while

wire feed speed and welding current predominantly influenced hardness. The analysis of variance (ANOVA) confirmed that the optimal thermal input—achieved by balancing current, feed rate, and travel speed—resulted in superior metallurgical bonding and microstructural refinement.

The Artificial Neural Network (ANN) model exhibited excellent predictive capability for both tensile strength and hardness, achieving mean absolute percentage errors (MAPE) below 1%, outperforming Taguchi and regression models. The high correlation coefficients ($R > 0.99$) demonstrated that the ANN effectively captured the nonlinear interdependencies among process parameters and mechanical responses. When integrated with the Genetic Algorithm (GA), the hybrid ANN–GA framework efficiently identified the global optimum at 85.3 A current, 7.7 m/min wire feed speed, and 3.8 mm/s welding speed, corresponding to predicted values of 242.5 MPa tensile strength and 108.4 HV hardness with an overall fitness of 0.935.

Experimental validation under slightly adjusted parameters confirmed the model's robustness, yielding average deviations of less than 1% between predicted and measured values. These results verify that the ANN–GA hybrid model provides a powerful and reliable tool for optimizing complex, nonlinear welding processes. Overall, this research establishes a data-driven framework that can be applied to other aluminum alloys and additive manufacturing systems to achieve high-strength, high-integrity components with reduced trial-and-error experimentation.

Acknowledgement

The authors would like to express their sincere gratitude to the Faculty of Industrial Technology, Nakhon Phanom University, for providing research facilities, laboratory instruments, and experimental equipment used throughout this study. Their continuous support and technical assistance were instrumental in the successful completion of this work.

References

[1] SARIKAYA, M., ÖNLER, D. B., DAĞLI, S., HARTOMACIOĞLU, S., GÜNAY, M., & KRÓLCZYK, G. M. (2024). A review on aluminum alloys produced by wire arc additive manufacturing (WAAM): Applications, benefits, challenges and future trends. In: *Journal of Materials Research and Technology*, Vol. 33, pp. 5643–5670.

[2] HAUSER, T., REISCH, R. T., BREESE, P. P., LUTZ, B. S., PANTANO, M., NALAM, Y., & KAPLAN, A. F. (2021). Porosity in wire arc additive manufacturing of aluminium alloys. In: *Additive Manufacturing*, Vol. 41, p. 101993.

[3] DAI, P., LI, A., ZHANG, J., CHEN, R., LUO, X., WEN, L., & LV, X. (2024). Research status and development trend of wire arc additive manufacturing technology for aluminum alloys. In: *Coatings*, Vol. 14, No. 9, p. 1094.

[4] SULAIMAN, S. K., ALKAHARI, M. R., JUZAILA ABD LATIF, M., HARANGAN PRASADA MANURUNG, Y., & PRIAPRATAMA PRAJADHIANA, K. (2025). Thermal Analysis of Micro Plasma Wire Arc Additive Manufacturing Deposition Process. In: *Manufacturing Technology*, Vol. 25, No. 3, pp. 396–404.

[5] LANGELANDSVIK, G., AKSELSEN, O. M., FURU, T., & ROVEN, H. J. (2021). Review of aluminum alloy development for wire arc additive manufacturing. In: *Materials*, Vol. 14, No. 18, p. 5370.

[6] TONELLI, L., LAGHI, V., PALERMO, M., TROMBETTI, T., & CESCHINI, L. (2021). AA5083 (Al–Mg) plates produced by wire-and-arc additive manufacturing: Effect of specimen orientation on microstructure and tensile properties. In: *Progress in Additive Manufacturing*, Vol. 6, No. 3, pp. 479–494.

[7] CHARDE, M. M., BHALERAO, Y. J., CEPOVA, L., RASHINKAR, S. N., & SWARNA, B. (2025). AI-Integrated Thermal Prediction and Multi-Criteria Optimization in Cylindrical Grinding Using Machine Learning and Genetic Algorithms. In: *Manufacturing Technology*, Vol. 25, No. 4, pp. 432–447.

[8] LUSI, N., FIVERIATI, A., AFANDI, A., GUSTI NGURAH BAGUS CATRA WEDARMA, I., YULIANDOKO, H., DARSIN, M., & QUTABA, S. (2023). Predictive modelling on machining performance of ECDM using artificial neural network and particle swarm optimization. In: *Manufacturing Technology*, Vol. 23, No. 5, pp. 649–662.

[9] KIM, J. Y., LEE, D. Y., LEE, J., & LEE, S. H. (2021). Parameter optimization of hybrid-tandem gas metal arc welding using analysis of variance-based Gaussian process regression. In: *Metals*, Vol. 11, No. 7, p. 1087.

[10] KONG, C., SOFI, A. Z. M., & MAMAT, S. (2024). Advancements and challenges in wire arc additive manufacturing – a review. In: *Malaysian Journal of Bioengineering and Technology*, Vol. 1, No. 2, pp. 130–136.

[11] KIM, G. G., KIM, D. Y., HWANG, I., KIM, D., KIM, Y. M., & PARK, J. (2021). Mechanical properties of aluminum 5083 alloy GMA welds with different magnesium and manganese content of filler wires. In: *Applied Sciences*, Vol. 11, No. 24, p. 11655.

[12] SHAH, A., ALIYEV, R., ZEIDLER, H., & KRINKE, S. (2023). A review of the recent developments and challenges in wire arc additive manufacturing (WAAM) process. In: *Journal of Manufacturing and Materials Processing*, Vol. 7, No. 3, p. 97.

[13] ASTM INTERNATIONAL. (2021). ASTM E8/E8M-21 Standard Test Methods for Tension Testing of Metallic Materials. In: *ASTM Standards*.

[14] INSTRON. (2019). The Definitive Guide to Metals Tensile Testing to ASTM E8 and A370. In: *Instron Technical Manual*.

[15] ASTM INTERNATIONAL. (2017). ASTM E384-17 Standard Test Method for Microindentation Hardness of Materials. In: *ASTM Standards*.

[16] KUMAR, V., SAHU, D. R., & MANDAL, A. (2022). Parametric study and optimization of GMAW-based AM process for multi-layer bead deposition. In: *Materials Today: Proceedings*, Vol. 62, pp. 255–261.

[17] CASARINI, A., COELHO, J. P., OLÍVIO, É. T., BRAZ-CÉSAR, M., & RIBEIRO, J. (2020). Optimization and influence of GMAW parameters for weld geometrical and mechanical properties using the Taguchi method and variance analysis. In: *KnE Engineering*, pp. 781–794.

[18] YENIYIL, E., YILDIZ, H., ÜLKER, A., ERBAYTAN, D., & SAYER, S. (2025). Process optimization of double-pulsed GMAW using the Taguchi method for enhanced tensile strength. In: *Results in Engineering*, p. 106696.

[19] VERMA, R. P., PANDEY, K. N., & MITTAL, G. (2024). Genetic-neural optimization approach for gas metal arc welding of dissimilar aluminium alloys of AA5083-O/AA6061-T6. In: *International Journal of Lightweight Materials and Manufacture*, Vol. 7, No. 1, pp. 214–220.

[20] NAKOWONG, K., SUWANNASOPA, D., KAEWCHALUN, A., LAMWONG, J., & POOKAMNERD, Y. (2025). A genetic-neural optimization approach for friction stir spot welding of semi-solid metal aluminum alloy 5083. In: *Engineering and Applied Science Research*, Vol. 52, No. 5, pp. 541–550.

[21] WAN, Z., YI, Z., ZHAO, Y., ZHANG, S., LI, Q., LIN, J., & WU, A. (2024). Prediction and optimization of tensile properties of 2219-T8 aluminum alloy TIG welding joint by machine learning. In: *Materials & Design*, Vol. 245, p. 113274.

[22] JEET, S., BARUA, A., PARIDA, B., SAHOO, B. B., & BAGAL, D. K. (2018). Multi-objective optimization of welding parameters in GMAW for stainless steel and low carbon steel using hybrid RSM-TOPSIS-GA-SA approach. In: *International Journal of Technical Innovation in Modern Engineering & Science*, Vol. 4, pp. 683–692.

[23] CHAUDHARI, R., BHATT, R., VAGHASIA, V., RAJA, B. D., PATEL, V. K., KHANNA, S., & PATEL, V. V. (2023). A parametric study and experimental investigations of microstructure and mechanical properties of multi-layered structure of metal core wire using wire arc additive manufacturing. In: *Journal of Advanced Joining Processes*, Vol. 8, p. 100160.

[24] DAHAT, S., HURTIG, K., ANDERSSON, J., & SCOTTI, A. (2020). A methodology to parameterize wire + arc additive manufacturing: a case study for wall quality analysis. In: *Journal of Manufacturing and Materials Processing*, Vol. 4, No. 1, p. 14.

[25] PANAGIOTOPOULOS, V., HADJIPANTELIS, N., & GANTES, C. J. (2025, October). Influence of process parameters on weld quality and nominal geometry of wire arc additively manufactured steel elements. In: *Structures*, Vol. 80, p. 110044.

[26] DINOVITZER, M., CHEN, X., LALIBERTE, J., HUANG, X., & FREI, H. (2019). Effect of wire and arc additive manufacturing (WAAM) process parameters on bead geometry and microstructure. In: *Additive Manufacturing*, Vol. 26, pp. 138–146.

[27] GIERTH, M., HENCKELL, P., ALI, Y., SCHOLL, J., & BERGMANN, J. P. (2020). Wire arc additive manufacturing (WAAM) of aluminum alloy AlMg5Mn with energy-reduced gas metal arc welding (GMAW). In: *Materials*, Vol. 13, No. 12, p. 2671.

[28] WANG, S., GU, H., WANG, W., LI, C., REN, L., WANG, Z., & MA, P. (2020). The influence of heat input on the microstructure and properties of wire-arc-additive-manufactured Al-Cu-Sn alloy deposits. In: *Metals*, Vol. 10, No. 1, p. 79.

[29] GARAŠIĆ, I., ŠTEFOK, M., JURICA, M., SKEJIĆ, D., & PERIĆ, M. (2025). Mechanical properties analysis of WAAM-produced wall made from 6063 alloy using AC MIG process. In: *Applied Sciences*, Vol. 15, No. 12, p. 6740.

[30] HABIB, N., VAFADAR, A., & GUZZOMI, F. (2025). A comparative study of aluminium properties manufactured using additive friction stir deposition (AFSD) and wire arc additive manufacturing (WAAM). In: *Progress in Additive Manufacturing*, pp. 1–21.

[31] KOUL, P., & SIDDARAMU, Y. (2025). A review of wire arc additive manufacturing. In: *International Journal of Scientific Research in Modern Science and Technology*, Vol. 4, No. 8, pp. 1–32.

[32] WANG, X., LIU, L., ZHOU, C., XU, T., LUO, M., & HU, X. (2023). Dynamic control of aluminum morphology by wire and arc additive manufacturing based on image feedback. In: *Frontiers in Materials*, Vol. 10, p. 1220202.

[33] VORA, J., PARIKH, N., CHAUDHARI, R., PATEL, V. K., PARAMAR, H., PIMENOV, D. Y., & GIASIN, K. (2022). Optimization of bead morphology for GMAW-based wire-arc additive manufacturing of 2.25Cr-1.0Mo steel using metal-cored wires. In: *Applied Sciences*, Vol. 12, No. 10, p. 5060.

[34] RIFFEL, K. C., BAWA, R., CHAN, J., ADHAMI, R., GOFMAN, D., & RAMIREZ, A. J. (2025). Artificial intelligence and statistical mapping applied to additive manufacturing toolpath optimization in wire-arc DED. In: *Integrating Materials and Manufacturing Innovation*, pp. 1–17.

[35] DU, W., SUN, G., LI, Y., & CHEN, C. (2023). Process optimization, microstructure and mechanical properties of wire arc additive manufacturing of aluminum alloy by using DP-GMAW based on response surface method. In: *Materials*, Vol. 16, No. 16, p. 5716.

[36] KAPANOVA, K. G., DIMOV, I., & SELLIER, J. M. (2018). A genetic approach to automatic neural network architecture optimization. In: *Neural Computing and Applications*, Vol. 29, No. 5, pp. 1481–1492.

[37] SAGAR, P. (2025). Hybrid GA-ANN and GA-ANFIS soft computing approaches for optimizing tensile strength in magnesium-based composites fabricated via friction stir processing. In: *Materials Today Communications*, Vol. 44, p. 112083.

[38] TAGIMALEK, H., MARAKI, M. R., MAHMOODI, M., MOGHADDAM, H. K., & FARZAD-RIK, S. (2022). Prediction of mechanical properties and hardness of friction stir welding of Al 5083/pure Cu using ANN, ICA and PSO model. In: *SN Applied Sciences*, Vol. 4, No. 4, p. 102.

[39] LUESAK, P., PITAKASO, R., SETHANAN, K., GOLINSKA-DAWSON, P., SRICHOK, T., & CHOKANAT, P. (2023). Multi-objective modified differential evolution methods for the optimal parameters of aluminum friction stir welding processes of AA6061-T6 and AA5083-H112. In: *Metals*, Vol. 13, No. 2, p. 252.

[40] MEYVECI, A., KARACAN, I., DURMUŞ, H., & ÇALIGÜLÜ, U. (2012). Artificial neural network (ANN) approach to hardness prediction of aged aluminium 2024 and 6063 alloys. In: *Materials Testing*, Vol. 54, No. 1, pp. 36–40.

[41] LE, V. T., DOAN, Q. T., MAI, D. S., BUI, M. C., TRAN, H. S., VAN TRAN, X., & NGUYEN, V. A. (2022). Prediction and optimization of processing parameters in wire and arc-based additively manufacturing of 316L stainless steel. In: *Journal of the Brazilian Society of Mechanical Sciences and Engineering*, Vol. 44, No. 9, p. 394.

[42] LOVE, A., VALDEZ PASTRANA, O. A., BEHSERESHT, S., & PARK, Y. H. (2025). Advancing metal additive manufacturing: A review of numerical methods in DED, WAAM, and PBF. In: *Metrology*, Vol. 5, No. 2, p. 30.

[43] OMIYALE, B. O., OLUGBADE, T. O., ABIOYE, T. E., & FARAYIBI, P. K. (2022). Wire arc additive manufacturing of aluminium alloys for aerospace and automotive applications: A review. In: *Materials Science and Technology*, Vol. 38, No. 7, pp. 391–408.

[44] WAQAS, A., QIN, X., XIONG, J., WANG, H., & ZHENG, C. (2019). Optimization of process parameters to improve the effective area of deposition in GMAW-based additive manufacturing and its mechanical and microstructural analysis. In: *Metals*, Vol. 9, No. 7, p. 775.

[45] WANG, C., BAI, H., REN, C., FANG, X., & LU, B. (2020, October). A comprehensive prediction model of bead geometry in wire and arc additive manufacturing. In: *Journal of Physics: Conference Series*, Vol. 1624, No. 2, p. 022018.

[46] ROHANINEJAD, M., TAVAKKOLI-MOGHADDAM, R., VAHEDI-NOURI, B., HANZÁLEK, Z., & SHIRAZIAN, S. (2022). A hybrid learning-based meta-heuristic

algorithm for scheduling of an additive manufacturing system consisting of parallel SLM machines. In: *International Journal of Production Research*, Vol. 60, No. 20, pp. 6205–6225.

[47] REDDY, B. V. S., SHAIK, A. M., SASTRY, C. C., KRISHNAIAH, J., BHISE, C. A., & RAMAKRISHNA, B. (2024). Machine learning approaches for predicting mechanical properties in additive manufactured lattice structures. In: *Materials Today Communications*, Vol. 40, p. 109937.

[48] NAGESH, D. S., & DATTA, G. L. (2008). Modeling of fillet welded joint of GMAW process: Integrated approach using DOE, ANN and GA. In: *International Journal on Interactive Design and Manufacturing (IJIDeM)*, Vol. 2, No. 3, pp. 127–136.

[49] MOMENI, E., NAZIR, R., ARMAGHANI, D. J., & MAIZIR, H. (2014). Prediction of pile bearing capacity using a hybrid genetic algorithm-based ANN. In: *Measurement*, Vol. 57, pp. 122–131.

[50] MOHAMAD, E. T., FARADONBEH, R. S., ARMAGHANI, D. J., MONJEZI, M., & MAJID, M. Z. A. (2017). An optimized ANN model based on genetic algorithm for predicting ripping production. In: *Neural Computing and Applications*, Vol. 28, Suppl. 1, pp. 393–406.

[51] LI, Y., JIA, M., HAN, X., & BAI, X. S. (2021). Towards a comprehensive optimization of engine efficiency and emissions by coupling artificial neural network (ANN) with genetic algorithm (GA). In: *Energy*, Vol. 225, p. 120331.

[52] NAGESH, D. S., & DATTA, G. L. (2010). Genetic algorithm for optimization of welding variables for height-to-width ratio and application of ANN for prediction of bead geometry for TIG welding process. In: *Applied Soft Computing*, Vol. 10, No. 3, pp. 897–907.

[53] EQUBAL, A., SHAMIM, M., BADRUDDIN, I. A., EQUBAL, M. I., SOOD, A. K., NIK GHAZALI, N. N., & KHAN, Z. A. (2020). Application of the combined ANN and GA for multi-response optimization of cutting parameters for the turning of glass fiber-reinforced polymer composites. In: *Mathematics*, Vol. 8, No. 6, p. 947.